17

Practical Considerations in the Selection and Application of Fluorescent Probes

Iain D. Johnson

INTRODUCTION

Due to its sensitivity, multiplexing capacity, and applicability to live specimens, fluorescence is the dominant contrast mechanism used in three-dimensional (3D) biological microscopy. Use of fluorescence detection generally requires specimens to be labeled with extrinsic probes. This is because most biological molecules and structures of interest are not intrinsically fluorescent in spectral ranges that are useful for detection, and even those that are cannot usually be discriminated from each other on the basis of their intrinsic fluorescence. Extrinsic labeling circumvents these problems at the expense of introducing others. Extrinsic probes must be delivered to the region of interest and remain there for long enough to acquire the experimental data. Once *in situ*, the probe should ideally be a passive reporter that does not induce significant perturbations of the biological structure or function that we wish to study. Furthermore, the detection process itself may have deleterious side effects in the form of photobleaching and photoxicity, resulting from the interaction of excitation light with the probe and the specimen.

Based on the premise that understanding probe behavior is a key component in evaluating the information content of images obtained using fluorescence microscopy, this chapter reviews the practical considerations involved in probe selection and use. In Table 17.1, fourteen key characteristics of probes and specimens are listed in relation to their impact on labeling and detection processes. The ordering of topics in Table 17.1 reflects the sequence of discussion in subsequent sections of this chapter.

SELECTION CRITERIA FOR DYES AND PROBES

A fluorescent dye (or, synonymously, a fluorophore) is a fluorescent molecule that does not associate with any particular biological target. A fluorescent probe is a dye that has been modified in some way to detect specific biological targets (Fig. 17.1). Targets include specific groups of cells in a tissue, organelles, proteins, nucleic acids, ions (Ca^{2+}, Mg^{2+}, H^+, Na^+, etc.) and enzymes. From this perspective, fluorescein is a **dye** whereas fluorescein-labeled proteins and peptides are **probes**. Similarly, the green fluorescent protein (GFP) can be considered to be a "dye" and GFP fusion proteins are probes. In some cases, the structural characteristics of the dye itself are sufficient to confer biospecificity. For example, cationic dyes such as MitoTracker Red CMXRos, JC-1, and rhodamine 123 stain mitochondria driven by the internally negative membrane potential. Dyes and probes have both biochemical and spectroscopic properties. Biochemical properties determine the molecular association, transport, and metabolic fate of the probe. Examples include water solubility, membrane permeability, receptor binding affinity, and enzymatic conversion rates. Spectroscopic properties primarily determine the number and energy distribution of photons available for detection. They include excitation and emission spectra, molar absorptivity (extinction coefficient), fluorescence quantum yield, and photobleaching rate.

Organic Dyes

Fluorescein and its derivatives (Fig. 17.1) have been the most widely used class of organic dyes used as fluorescent probes. Their utility is derived in part from the fact that fluorescein is efficiently excited by the 488 nm argon-ion laser line. Coumarins and rhodamines have been the primary blue (~450 nm) and orange (~580 nm) emitting dyes used alongside fluorescein (green emission, ~520 nm) in two-color labeling applications. Each class has some significant disadvantages. Fluoresceins are pH sensitive and highly susceptible to photobleaching. Rhodamines have a tendency to aggregate in aqueous solutions resulting in self-quenching of fluorescence (see below). Coumarins have relatively low excitation efficiencies — ε_{max} ~ 20,000 $M^{-1}cm^{-1}$ compared to ε_{max} ~ 100,000 $M^{-1}cm^{-1}$ for fluoresceins and rhodamines. Coumarins also have other drawbacks associated with ultraviolet excitation, namely, phototoxicity and a requirement for expensive quartz optical components. These latter problems can be circumvented by use of two-photon excitation.

The deficiencies of fluorescein, rhodamine, and coumarin dyes have spurred the development of new dye classes that have been deliberately optimized for biomolecular detection applications. Three of these classes will be discussed here (in alphabetical order) — AlexaFluor dyes, BOPIDY dyes, and cyanine (Cy) dyes (Table 17.2). The AlexaFluor dye series has 19 members with excitation maxima matched to principal laser output lines between 350 and 750 nm (Fig. 17.2). The AlexaFluor dyes are more water-soluble than their fluorescein and rhodamine counterparts, resulting directly or indirectly in reduced levels of self-quenching upon coupling to proteins and improved photostability (Panchuk-Voloshina *et al.*,1999; Berlier *et al.*, 2003). The Cy dye series (Mujumdar *et al.*, 1993) has fewer excitation wavelength variants but contains similar design elements to the AlexaFluor dyes series — sulfonic acid substituents to increase aqueous solubility and the use of *N*-hydroxysuccinimidyl (NHS) ester reactive chemistry for cou-

Iain D. Johnson • Molecular Probes, Inc., Eugene, Oregon 97402

TABLE 17.1. Key Characteristics of Probes and Specimens

Property	Significance
1. Excitation spectrum	Should be wavelength-matched with instrument source output for optimum fluorescence excitation efficiency (see Fig. 17.2).
	Overlap with donor emission spectrum required for FRET.
2. Extinction coefficient (ε; units $M^{-1}cm^{-1}$)	Determining factor in fluorescence output per dye.
3. Emission spectrum	Ability to resolve probe signal from autofluorescence.
	Selection of probes for simultaneous imaging of multiple targets.[a]
	Overlap with acceptor excitation spectrum required for FRET.
4. Fluorescence quantum yield (QY)	Determining factor in fluorescence output per dye. Often environment dependent.
5. Environment sensitivity	Impacts the proportionality of dye fluorescence to concentration.
6. Probe size/permeability/solubility	Impacts choice of loading method.
7. Specimen type (single cell, cell population, tissue)	Impacts choice of loading method.
8. Target abundance	Determines total fluorescence output. May compel use of signal amplification techniques[b] or GFP overexpression.
9. Autofluorescence	Impacts selection of excitation/emission wavelength ranges and level of labeling required.
10. Probe localization	Localized accumulations are more readily detectable than the diffuse distributions.
11. Probe metabolism and retention	Determines stability of labeling.
12. Probe-mediated cytotoxicity	Impacts specimen viability.
	May require reduced loading concentration and/or selecting a different probe.
13. Photobleaching	May necessitate attenuation of excitation power.
	Determines ability to conduct time-lapse experiments.
14. Phototoxicity	Impacts specimen viability.

[a] Dyes with narrow emission bandwidths are preferred for minimizing spillover of the signal into adjacent detection channels (see Fig. 17.2).
Probes that exhibit environment-dependent spectral shifts, such as the JC-1 and BOPIDY FL ceramide are difficult to employ in these applications for this reason.
[b] See Wang and colleagues (1999) for example.

pling to free amine groups on proteins and other biomolecules [Fig. 17.3(A)]. In contrast to the AlexaFluor and Cy dye series, BOPIDY dyes are non-polar and relatively insoluble in water [Fig. 17.3(B)]. Instead of protein labeling, they are primarily utilized in fluorescent lipid analogs (Pagano *et al*., 2000; Farber *et al*., 2001) and analogs of receptor ligands such as nucleotides, steroids, alkaloids, and peptides (Daly and McGrath, 2003).

Environmental factors including pH, solvent polarity, binding to proteins, and dye–dye interactions can exert strong influences on dye fluorescence. Susceptibility to environment varies widely among dye classes. Dyes that are designed primarily for covalent labeling of proteins and nucleic acids such as AlexaFluor dyes and Cy dyes are highly fluorescent in water and retain similar levels of fluorescence after coupling. In histochemical and cytochemical

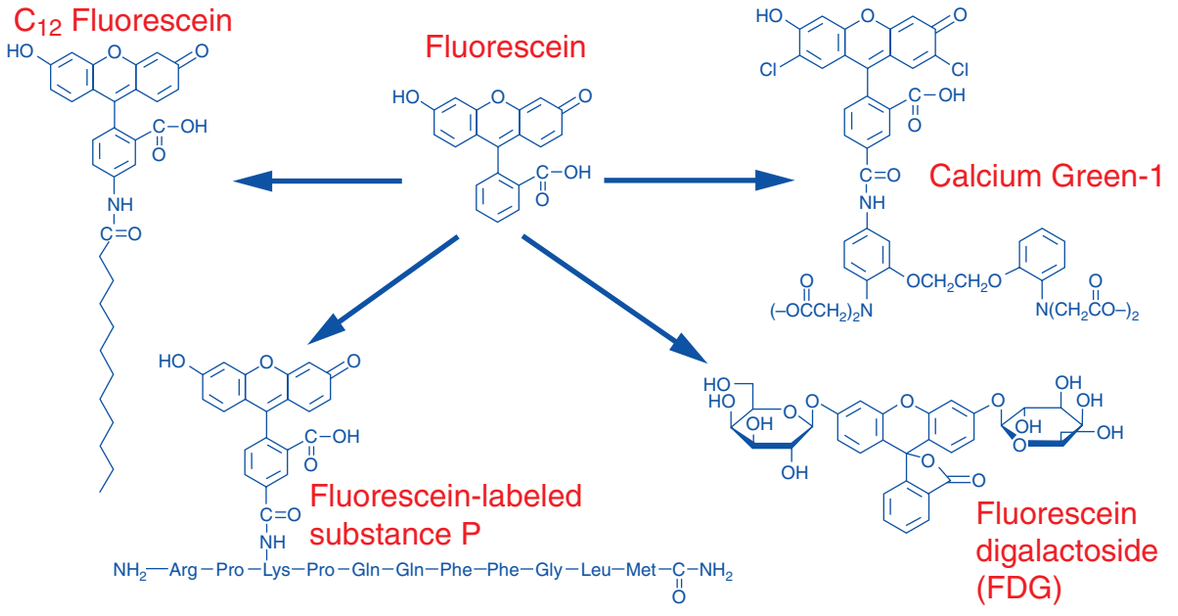

FIGURE 17.1. Derivatization of a fluorescent dye (fluorescein) to obtain target-specific response or localization characteristics. Clockwise from top left: The dodecanoyl (C_{12}) substituent of C_{12} fluorescein results in membrane localization. The intracellular Ca^{2+} indicator Calcium Green-1 consists of dichlorofluorescein coupled to the Ca^{2+}-selective chelator BAPTA. Fluorescein digalactoside (FDG) is a β-galactosidase activity sensor that generates an enzyme–dependent fluorescence intensity increase upon cleavage of the 3′- and 6′-galactose residues. Fluorescein-labeled substance P is a probe for neuropeptide receptors prepared by coupling 5-carboxyfluorescein, NHS-ester to the ε-amino group of lysine via the reaction chemistry outlined in Figure 17.3(D).

TABLE 17.2. Major Dye Classes

Dye Class	Examples	Brightness[a]	Environment Sensitivity[b]	Photostability	Biocompatability[c]	Two-Photon
Coumarin	AlexaFluor 350	+	+ + + +	+	+ + +	+
Fluorescein	FITC, calcein AM, CFSE[d]	+ + +	+ + + +	+	+ + +	+ +
BOPIDY	BOPIDY FL, BOPIDY TR	+ + +	+ + +	+ +	+ + + +	+ +
Phycobiliproteins	R-phycoerythrin (R-PE)	+ + + +	+ +	+ +	+ +	+ + + +
AlexaFluor	AlexaFluor 488, AlexaFluor 568, AlexaFluor 594, AlexaFluor 647	+ + + +	+ +	+ + + +	+ + + +	+ + +
Quantum dots	Qdot 605, Qdot 655	+ + + + +	+	+ + + + +	+	+ + + + +
Cyanines	Cy3, Cy5, DiI ($DiIC_{18}(3)$), $DiOC_6(3)$	+ + +	+ +	+ + + +	+ + +	+
Styryl dyes	FM 1-43, FM 4-64, Di-8-ANEPPS	+ +	+ + + + +	+ +	+ + +	+ + +
Rhodamines	TRITC, TMRE[e], Rhodamine 123	+ + +	+ + +	+ + + +	+ +	+ + +
Fluorescent proteins	ECFP, EGFP, EYFP, dsRed	+ +	+ +	+ +	+ + + + +	+ +

[a] Approximate representation of the product of molar extinction coefficient and fluorescence quantum yield. In cellular imaging applications, this will be heavily weighted by concentration (target abundance, expression level) and localization factors that are discussed in the text but are not included in this consideration.
[b] Assessment of the extent to which brightness is modulated by factors such as pH, aqueous exposure, dye interactions etc.
[c] A compound assessment of factors such as cytotoxicity, ease of delivery, and extent to which the dye modifies the structure and behavior of molecules to which it is attached. GFP has the highest rating because it is the only dye class of entirely biosynthetic origin.
[d] CFSE, carboxyfluorescein diacetate, succinimidyl ester.
[e] TMRE, tetramethylrhodamine ethyl ester.

applications, the lack of environmental sensitivity of these dyes is advantageous, as fluorescence images of their distribution are not biased by environment-dependent factors. Other classes such as styryl dyes (e.g., FM 1-43, FM 4-64) and many non-covalent nucleic acid stains (e.g., DAPI, TO-PRO-3, propidium iodide) are essentially non-fluorescent in water and only fluoresce when bound to their respective targets (membrane surfaces and DNA). In this case, unbound dyes are undetectable and the need to perform wash steps to remove them prior to imaging is therefore eliminated.

Within the confines of a cell, dyes frequently come into close spatial proximity with each other, resulting in dye–dye interactions. Attachment of multiple copies of fluorescein or rhodamine dyes to a single protein molecule usually results in the formation of dimers or higher aggregates of the dye that absorb but do not fluoresce. The process is commonly referred to as self-quenching. Dye aggregation is signified by peaks or shoulders in the absorption spectrum of the labeled protein that are not replicated in the fluorescence excitation spectrum, and also by changes in the circular dichroism spectrum (Mercola *et al*., 1972). Self-quenching produces the counterintuitive but sometimes useful result of fluorescence output decreasing as dye concentration increases. This is clearly detrimental if one is attempting to increase the fluorescent brightness of a protein by labeling it more heavily. Therefore, AlexaFluor dyes and Cy dyes are designed to avoid self-quenching by incorporating negatively charged sulfonic acid substituent groups that produce mutual electrostatic repulsion and increased water solubility (Fig. 17.3). Self-quenching can be exploited to advantage for detection of proteolytic activity by preparation of protein conjugates that are deliberately over-labeled. Probes of this type allow *in situ* localization of enzymatic activity in tissues (Mook *et al*., 2003) and organisms (Farber *et al*.,

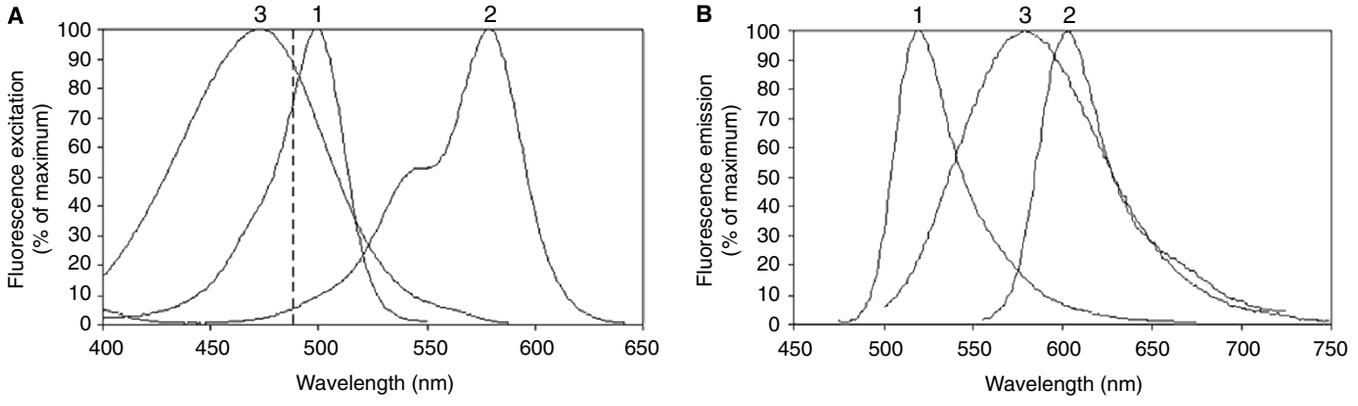

FIGURE 17.2. (A) Matching microscope excitation source outputs to dye spectra. Fluorescence excitation spectra of AlexaFluor 488 (1), AlexaFluor 568 (2), and FM 1-43 (3) dyes relative to the 488 nm argon-ion laser line (shown by the vertical dashed line). Due to the relatively inefficient excitation of the AlexaFluor 568 dye at 488 nm, it is not suitable for multiplex labeling in combination with FM 1-43 or AlexaFluor 488 nm dyes unless the microscope is also equipped with a 568 nm krypton-ion laser or 561 nm diode-pumped solid state laser. (B) Emission overspill considerations in multicolor detection. The wide emission spectral bandwidth of FM 1-43 (3) results in substantial overlap with both AlexaFluor 488 (1) and AlexaFluor 568 (2) dyes, making discrimination by means of wavelength filtering difficult to achieve. The AlexaFluor 488 and AlexaFluor 568 dyes are spectrally well resolved. Note, however, that the relative amplitudes of the spectra shown in the figure would only pertain in a real experimental situation if the dyes were excited with equal efficiency and were present at equal concentrations within the field of view.

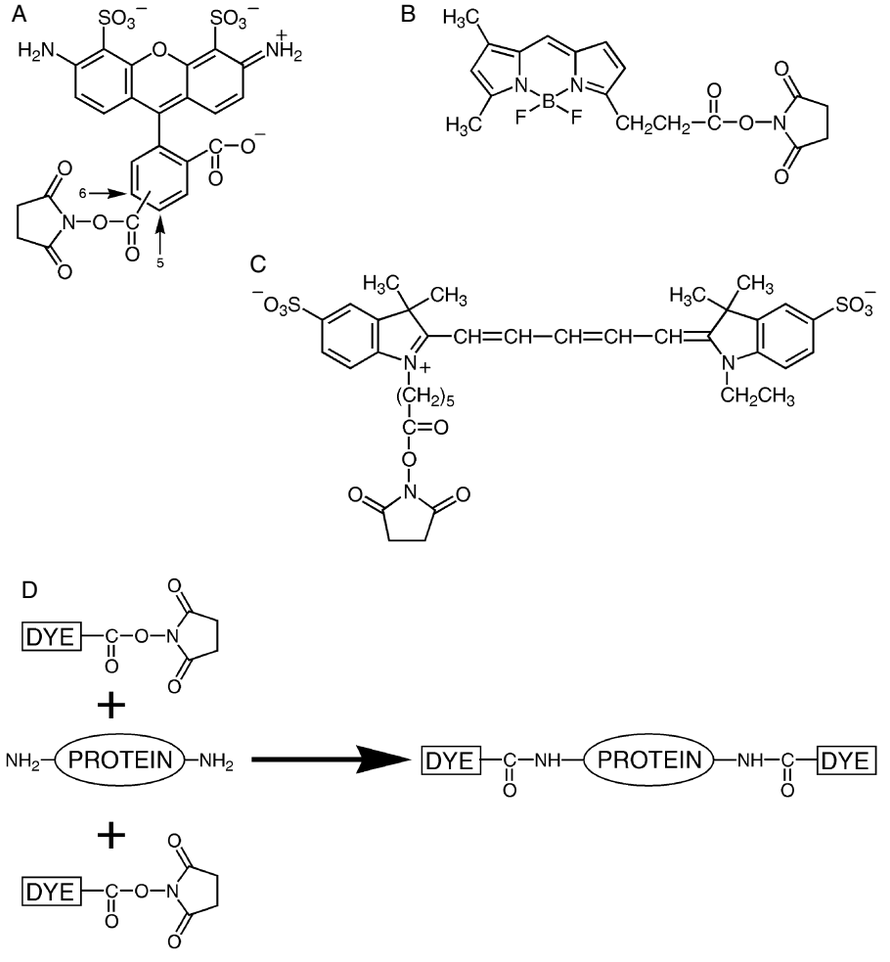

FIGURE 17.3. (A) Structures of amine-reactive dyes. (A) AlexaFluor 488, NHS ester; (B) BOPIDY FL, NHS ester; (C) Cy5, NHS ester (NHS = *N*-hydroxysuccinimidyl). (D) Reaction of a dye–NHS ester with protein amino groups yielding a stable carboxamide-linked conjugate.

2001). Fluorescent proteins and quantum dots have much less intrinsic environmental sensitivity than organic dyes because in both cases the fluorophore is encapsulated within one or more insulating layers. They are therefore more difficult to adapt for local environment sensing applications of the type described above. To do so, it is necessary to make use of fluorescence resonance energy transfer (FRET; Jales-Erijman and Jovin, 2003), a type of dye–dye interaction with a longer effective range than those responsible for self-quenching.

Stable coupling of organic dyes to proteins, nucleic acids, and other biomolecules can be accomplished using several well-characterized reaction chemistries. Currently, the most widely used method is the reaction of NHS ester dye derivatives with amines (e.g., ε–NH_2 of lysine) to form stable carboxamide linkages [Fig. 17.3(D)]. The principal alternative coupling method is reaction of iodoacetamide or maleimide derivatives of dyes with cysteine sulfhydryl groups to form thioether linkages. Textbook-level descriptions of these and other coupling chemistries may be consulted for further details (Hermanson, 1996; Haugland, 2002). Labeling protocols generally require some degree of protein-specific optimization with respect to the dye:protein ratio. This is merely a reflection of the fact that proteins vary widely in size and in the number and distribution of reactive targets. Typically, no more than about three to five dyes can be attached per protein without self-quenching of fluorescence and/or inactivating the protein. Note that degree-of-labeling values, as conventionally determined by absorption measurements, are sample averages. A preparation with an average of n dyes per protein will contain a range of labeling stoichiometries (. . . $n-2$, $n-1$, n, $n+1$, $n+2$ . . . etc.) that can be resolved by capillary electrophoresis or MALDI-TOF mass spectrometry (Lu and Zenobi, 2000). Furthermore, because the labeling reactions are indiscriminate with respect to the location of the target amino acid residue, labeling in a site that is critical for activity or binding may result in an inactive conjugate (Adamczyk *et al*., 1999). In these cases, activity can be preserved by performing the labeling reaction with the active site blocked by addition of its cognate substrate or ligand (Ramjeesingh *et al*., 1990).

Fluorescent Proteins: Green Fluorescent Protein and Phycobiliproteins

The cloning and heterologous expression of the *Aequoria victoria* green fluorescent protein in 1994 has had an immense impact on fluorescence microscopy of living cells in the past decade. There are many excellent review articles (Tsien, 1998; Zhang *et al*., 2002; Lippincott-Schwartz and Patterson, 2003) and entire books (Chalfie and Kain, 1998; Sullivan and Kay, 1999) devoted to the

properties and applications of GFP. Only selected points setting GFP in relation to other fluorescent labeling technologies will be considered here. The spectroscopic properties of GFP and its variants are unexceptional (ε_{max} ~ 53,000 $M^{-1}cm^{-1}$, QY ~ 0.6 for the most frequently used variant, EGFP (Patterson *et al*., 1997). However, the extraordinary utility of GFP resides in its biochemical properties — more specifically, in the ability to construct fusion proteins at the DNA level and express these in an almost unlimited range of cell types, tissues, and organisms. In principal, information on intracellular protein localization that has traditionally been obtained using dye-labeled antibodies in fixed cells can now be obtained in living cells, with the added dimension of following translocation processes in real time as opposed to observing only their end-points. Accurate localization of GFP fusion proteins relative to their native counterparts is clearly an essential prerequisite for these applications. GFP is a small protein (molecular weight ~27 kDa) consisting of 11 β-strands forming a hollow cylinder approximately 4.2 nm in length by 2.4 nm in diameter that encapsulate the *p*-hydroxybenzylideneimidazolidinone fluorophore. These dimensions are relatively large compared to organic dyes that typically have molecular weights <1000 and are represented by a flat disk of ~1 nm diameter. Intracellular GFP concentrations are determined by a combination of factors including levels of gene expression and rates of posttranslational folding and proteolysis. The spontaneous cyclization reaction responsible for formation of the fluorophore from residues 65 to 67 (Ser-Tyr-Gly in the wild-type *A. victoria* protein) requires molecular oxygen. Thus, only 16% of wild-type GFP synthesized *in vitro* under conditions of limited oxygen availability is fluorescent, compared to 88% in the presence of abundant oxygen (Nemetz *et al*., 2001). Therefore, GFP fluorescence in hypoxic cells and tissues such as tumors may not accurately reflect the level of gene expression (Coralli *et al*., 2001). Site-directed mutagenesis of *A. victoria* GFP has generated variants with shifted excitation and emission spectra. The cyan (CFP) and yellow (YFP) variants are particularly useful for co-localization of proteins via FRET imaging (Siegel *et al*., 2000). Spectral coverage has been extended to the red range by cloning and expression of a fluorescent protein known as DsRed from *Discosoma* coral (Matz *et al*., 1999). Major re-engineering of DsRed has been undertaken to eliminate some undesirable characteristics including slow maturation and obligate tetramerization (Campbell *et al*., 2002).

Phycobiliproteins are a family of photosynthetic accessory proteins from cyanobacteria and eukaryotic algae. The most commonly used phycobiliprotein for biomolecular labeling applications, R-phycoerythrin is a large cylindrical protein with a molecular weight of 240 kDa and dimensions of 6 nm in length by 12 nm in diameter. Each molecule contains 34 tetrapyrrole chromophores attached to the polypetide backbone via thioether linkages. To fulfill their biological role of transferring energy from absorbed light to chlorophyll in the photosynthetic reaction center, the positioning of the chromophores within the protein structure has evolved to maximize the efficiency of both absorption and fluorescence. Due to its exceptional light harvesting capacity, R-phycoerythrin can be efficiently excited at 488 nm ($\varepsilon_{488\,nm}$ ~ 1,100,000 $M^{-1}cm^{-1}$) even though this is far from its absorption maximum of 565 nm. It is therefore well suited for single excitation/dual emission detection in combination with fluorescein, AlexaFluor 488, GFP and other dyes with emission peaks around 520 nm. Due to their large size, phycobiliproteins are difficult to deliver to intracellular targets and are primarily of value for detection of low-abundance cell-surface antigens. Heterologous expression of C-phycocyanin has been accomplished in *E. coli* (Tooley *et al*., 2001). This is a much more technically demanding endeavor than GFP expression because it requires co-expression of enzymes required for the biosynthesis of the tetrapyrrole chromophores from heme.

Techniques for targeting dyes to specific binding motifs on intracellular proteins that combine elements of entirely intracellular expression of intrinsically fluorescent proteins and extracellular labeling of purified proteins by amine-reactive NHS chemistry are now emerging. These techniques include tetracysteine motif-binding biarsenical ligands (FlAsH; Adams *et al*., 2002) and engineered intracellular receptor proteins that recognize dyes or dye-coupled haptens (Beste *et al*.; 1999; Farinas and Verkman, 1999).

Quantum Dots

In complete contrast to fluorescent proteins, quantum dots have outstanding spectroscopic properties, whereas their biochemical properties of large size and inorganic composition represent a considerable challenge in biomolecular labeling applications. Quantum dots typically consist of a spherical core of the semiconductor cadmium selenide (CdSe) surrounded by a zinc sulfide (ZnS) shell which is in turn surrounded by a hydrophilic polymer surface coating (Bruchez *et al*., 1998; Chan and Nie, 1998). As well as stabilizing the electronic excited state of the semiconductor, the ZnS shell also prevents release of cytotoxic cadmium from the core (Derfus *et al*., 2004). The hydrophilic coating confers water solubility and incorporates functional groups for crosslinking to antibodies, streptavidin, and other targeting groups. Overall, the trilaminar particles are about 4 to 10 nm in diameter, comparable in size to the phycobiliproteins. The fluorescence output of a single quantum dot has been estimated to be approximately equivalent to 20 rhodamine dye molecules, similar to that of R-phycoerythrin (Chan and Nie, 1998). Due to their predominantly inorganic composition, quantum dots are largely invulnerable to the oxidative photobleaching reactions that affect organic dyes and fluorescent proteins. The diameter of the semiconductor core determines the fluorescence emission range of the particle (wavelength increases with increasing size). The excitation spectra of quantum dots are essentially continuous whereas the emission spectra are narrow and symmetrical (Fig. 17.4). Quantum dots exhibit exceptionally high molar absorptivity — for example, $\varepsilon_{600\,nm}$ = 650,000 $M^{-1}cm^{-1}$ and $\varepsilon_{400\,nm}$ = 3,500,000 $M^{-1}cm^{-1}$ (Watson *et al*., 2003). Furthermore, their two-photon excitation cross-sections exceed those of conventional organic dyes by factors of 100 to 1000 (Larson *et al*., 2003). Because quantum dots are extremely flexible with respect to excitation wavelength, they are well suited for simultaneous immunofluorescence detection of multiple targets (Wu *et al*., 2003). Careful optimization of staining conditions (buffer composition, etc.) is necessary to minimize non-specific labeling. The size and composition of quantum dots generally limits the range of accessible targets to cell-surface antigens and receptors and targets that can be accessed via endocytosis or injection (Jaiswal *et al*., 2003; Wu *et al*., 2003; Ballou *et al*., 2004). Development of intracellular delivery techniques using peptide vectors has recently been reported (Mattheakis *et al*., 2004).

Multi-Photon Excitation

The advent of two-photon excitation microsopy (Denk *et al*., 1990) has added a new spectral dimension to fluorescence microscopy, in addition to the benefits of increased imaging depth and reduced phototoxicity that derive from the transparency of tissues to infrared excitation light and confinement of excitation to the focal

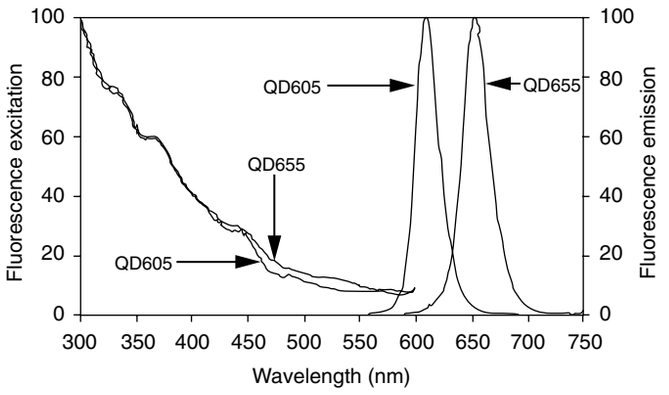

FIGURE 17.4. Fluorescence excitation and emission spectra of QD605–streptavidin and QD655–streptavidin (QD = quantum dot). The continuous and almost identical excitation spectra and the sharp, well-differentiated emission spectra contrast markedly with the corresponding characteristics of organic dyes [Fig. 17.2(A,B)].

plane (Zipfel *et al*., 2003a). Probes that were previously of limited utility in confocal microscopy due to their requirements for ultraviolet excitation, such as fura-2 (Ca^{2+}), SBFI (Na^{+}), monochlorobimane (glutathione), and DAPI (nuclear DNA), have acquired a new lease of life (Rose *et al*., 1999; Fricker and Meyer, 2001; Rubart *et al*., 2003). Furthermore, *in situ* imaging of small endogenous fluorophores such as serotonin and NADH, that are almost inaccessible to one-photon excitation, has now become practicable (Zipfel *et al*., 2003b; Rocheleau *et al*., 2004). With these exceptions, the collection of dyes and probes currently in use for two-photon excitation microscopy is largely the same as that employed in confocal and widefield fluorescence imaging. There are several published collections of two-photon excitation spectra and cross-sections that provide guidance on compatibility of dyes and probes with excitation sources (Xu and Webb, 1996; Xu *et al*., 1996; Bestvater *et al*., 2002; Dickinson *et al*., 2003). If two-photon spectral data is not available, the corresponding one-photon spectrum plotted on a doubled wavelength axis can be used as a first approximation. However two-photon excitation spectra differ from their one-photon counterparts to an extent that depends on the molecular orbital symmetry of the fluorophore (greater difference for higher symmetry fluorophores; Zipfel *et al*.,2003a). Consequently, most two-photon excitation spectra are blue shifted and broader compared to the corresponding one-photon spectra. Simply stated, a dye with a one-photon excitation peak at 500 nm will probably have a two-photon excitation maximum at <1000 nm (Ruthazer and Cline, 2002). In practice, most dyes with single-photon excitation maxima <600 nm can be effectively excited within the 700 nm to 1000 nm output range of the mode-locked titanium–sapphire laser sources used in the majority of two-photon excitation microscopes. In general, optimizing the excitation wavelength in relation to the peak of the dye excitation spectrum appears to be less critical than in the one-photon case.

INTRODUCING THE PROBE TO THE SPECIMEN

Loading Methods

After selecting a probe with appropriate biochemical and spectroscopic properties with regard to the experimental objectives and the microscope hardware to be used, the next task is to label the features of interest within the specimen. This is a relatively straightforward process in the fixed and permeabilized specimens used for immunofluorescence, for which there are well-established standard protocols (Brelje *et al*., 2002). The major practical concerns for immunolabeling of fixed specimens include antigen preservation and accessibility, non-specific binding and cross-reactivity of antibodies, and the potential for increased autofluorescence resulting from the chemical reactions used to achieve fixation (see also Chapter 18, *this volume*).

The permeability barriers and active metabolic processes of living cells and tissues present additional challenges for probe delivery and localization (Stephens and Pepperkok, 2001). Generally speaking, the severity of the intracellular delivery problem increases in proportion to the size of the probe and the complexity of the specimen (cell < tissue < whole organism). Ions are quite easy to deliver non-invasively via endogenous ion channels or using ionophores. Small organic dye-based probes are easy to moderately difficult, depending on their structural characteristics. For example, the rate of loading of the acetoxymethyl (AM) ester forms of intracellular Ca^{2+} indicators into intact frog muscle fibers decreases dramatically when their molecular weight exceeds about 850 (Zhao *et al*., 1997). In contrast, DAPI and lucifer yellow CH have similar molecular weights but can exhibit markedly different permeability through gap junctions due to their opposite electrostatic charges (Cao *et al*., 1998). Intracellular delivery of large probes such as phycobiliproteins, labeled antibodies, or quantum dots almost invariably requires invasive methods. An exception to the latter stipulation is GFP, which is synthesized and folded *in situ*, thereby eliminating the need for intracellular delivery except at the initial DNA transfection stage. Methods for transfection and expression of GFP will not be discussed here; detailed descriptions are available elsewhere (Sullivan and Kay, 1999; and in Chapter 45, *this volume*).

Several factors can be identified that influence loading method choices:

- Is the experimental specimen a pure or mixed cell culture or a tissue?
- If the specimen is multi-cellular, is disseminated (all cells) or selective (one cell or a subgroup of cells) loading desired?
- What is the size of the cells to be labeled?
- What is the size of the probe?
- Impact of loading on cell viability and function?
- Precision of amount delivered and location of delivery ("focal application")?

Before describing specific methods, a generally applicable guideline should be noted. Label the specimen to the minimum extent required to obtain the biological information that is sought. It is almost never desirable to increase fluorescence signals by increased dye loading or fluorescent protein expression. The following deleterious effects are all positively correlated with increased label concentration: phototoxicity, cytotoxicity, non-specific localization, and physiological or structural perturbation.

1. **Direct permeability:** This is the simplest of all techniques, involving nothing more than dispersing the probe in the extracellular medium and incubating for 5 to 60 minutes. It is generally applicable to neutral, monoanionic, and monocationic molecules with molecular weight <1000. Examples include JC-1, MitoTracker Red CMXRos, LysoTracker Red, BOPIDY FL ceramide, and $DiIC_{18}(3)$. Loading of lipophilic probes such as fluorescent lipid analogs (Tanhuanpaa and Somerharju, 1999) and acetoxymethyl (AM) esters (see item 3, below) is enhanced by the addition of

carriers and dispersing agents such as cyclodextrins, nonionic detergents (Pluronic F-127, Cremophor EL), and proteins such as bovine serum albumin (BSA). Also included in this general category are larger probe molecules that are taken up by endocytic processes such as dye-labeled transferrin conjugates.

2. **ATP-gated cation channels:** Provide a direct loading conduit for dyes with molecular weight <1000. Applicability restricted to cell types in which these channels are found (neurons and other sensory cells, dendritic cells, macrophages). Dyes to which this technique has been applied include FM 1-43 (Meyers *et al*., 2003), fura-2, and the pH indicator HPTS (pyranine; Gan *et al*., 1998).

3. **Membrane permeant esters:** An AM or acetate ester derivative of a polyanionic dye diffuses across the plasma membrane followed by intracellular release of free dye mediated by endogenous esterase activity (Fig. 17.5). The requirement for esterase activity imposes limitations on the cell types to which the technique can be applied, but provides a rapid and convenient method for uniform loading of adherent or suspended cells. Intracellular distribution of the dye can be manipulated to some extent by variations of temperature, dye structure, and incubation time (Lemasters *et al*., 1999), but cannot be precisely controlled (Fig. 17.5).

4. **Peptide-mediated uptake:** This relatively new technique is based on attachment of peptide vectors to molecular cargoes, which may be anything from small dyes to quantum dots (Mattheakis *et al*., 2004) or large (>100 kDa) proteins. The cellular uptake mechanism is not fully understood and remains under active investigation (Potocky *et al*., 2003). Efficacious peptide sequences (Fischer *et al*., 2001) consist of 8 to 30 amino acids with a preponderance of basic residues, and are largely derived from the proteins of infectious microorganisms. At present, this technique is far from being universally applicable and the attainable intracellular dye concentrations are rather low (10 to 100 n*M*; Waizenegger *et al*., 2002).

5. **Transient permeabilization:** Brief treatments of cells with low doses (≤0.1 mg/mL) of bacterial toxins (e.g., streptolysin O, staphylococcal α-toxin) or plant glycosides (β-escin, saponin) allows delivery of probes and other molecules. Although these treatments are easy to implement, the physiological integrity and viability of the cells is inevitably compromised to some extent. Walev and colleagues (2001) have provided a detailed analysis of the efficacy and collateral effects of streptolysin-O permeabilization of adherent and non-adherent cell types. The molecular weight cutoff for loading was found to be ~100,000 with intracellular concentrations of 10^5 to 10^6 molecules per cell.

6. **Osmotic permeabilization:** Similar to bacterial toxin permeabilization in applicability (non-selective loading of cell populations) and potential for compromising cellular integrity. Applicable to large proteins such as antibodies (Chakrabati *et al*., 1989).

7. **Electroporation:** Perhaps the most versatile technique currently available. Applicable to single cells (Haas *et al*., 2001), bulk loading of cell populations (Hashimoto *et al*., 1989), and focal

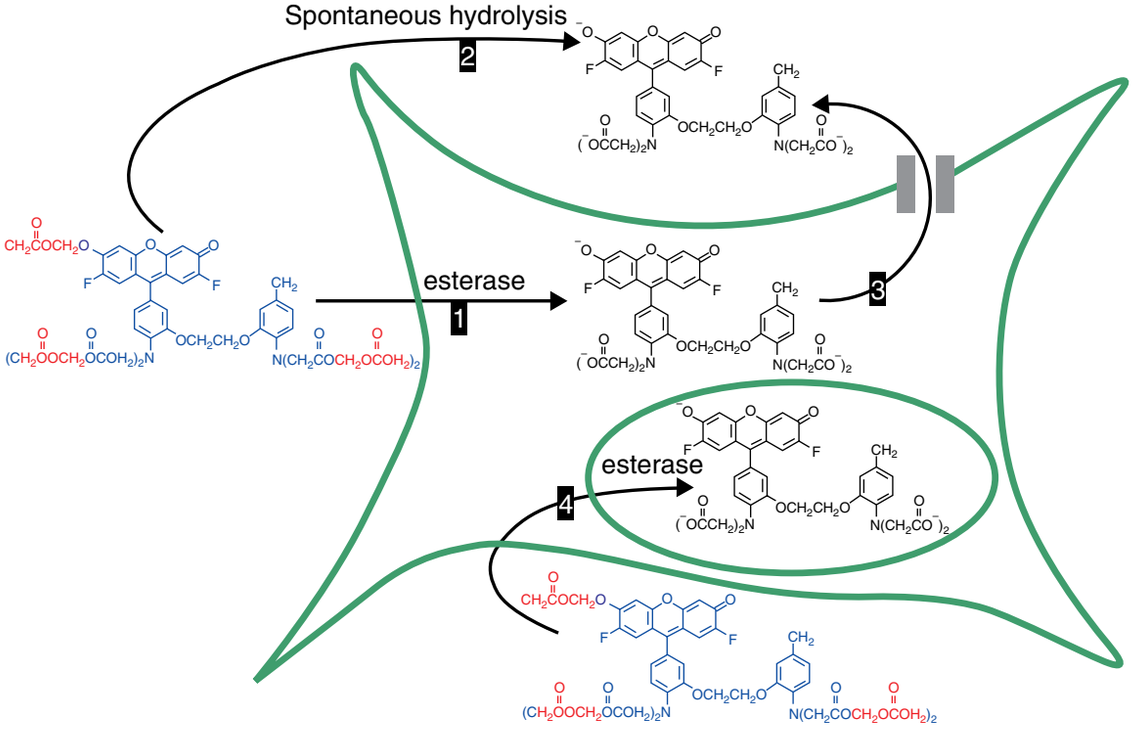

FIGURE 17.5. Cell loading with acetoxymethyl (AM) esters. The example shown represents the calcium indicator fluo-4. The intended objective of most measurements using fluo-4 is imaging of cytosolic Ca^{2+} dynamics. Loading of the dye via process (1), consisting of spontaneous permeation of the AM ester derivative of fluo-4 (shown in red and blue) across the plasma membrane followed by cleavage of the acetoxymethyl groups (red) by intracellular esterases is therefore the desired outcome. However, other dye transport processes may occur simultaneously. These include extracellular hydrolysis of the AM ester (2), extrusion of intracellular fluo-4 via organic anion transporters (3), and compartmentalization in membrane-enclosed organelles and vesicles (4). Processes (2–4) all result in fluorescence signals that are not responsive to cytosolic Ca^{2+} (see Fig. 17.6). The actual cellular labeling pattern obtained is determined by the relative rates of the permeation, transport, enzymatic, and chemical hydrolysis that contribute to pathways 1–4. These in turn are dependent on experimental variables such as cell type, cell viability, incubation medium composition, and temperature.

(spatially localized) delivery within tissues and organisms (Yasuda *et al*., 2000). Applicable to molecules large and small, from dyes and peptides up to antibodies (Marrero *et al*., 1995).

8. **Ballistic microprojectile (gene gun) delivery:** Primarily useful for labeling groups of cells deep (up to 300 µm) inside tissues. Widely used for transfection of GFP vectors in brain slices (O'Brien *et al*., 2001). Applications for loading neuronal tracers and intracellular calcium indicators have also been reported (Grutzendler *et al*., 2003).

9. **Microinjection:** Invasive, sequential (one cell at a time) but extremely precise. Provides exquisite control over the amount of probe delivered and in the selection of individual cells for labeling. Microinjection is quite demanding in terms of technical skill and instrumentation, and is difficult to apply to small cells (e.g., hepatocytes). Either pneumatic pressure or electrical current (iontophoresis) may be used as the driving force for injection. These two methods may produce significantly different cellular labeling results, even when they are applied to the same dye (Gerhardt and Palmer, 1987; Storms *et al*., 1998). Iontophoretic microinjection is restricted to electrostatically charged dyes such as lucifer yellow CH and AlexaFluor 594 hydrazide and is difficult to apply to large molecules (molecular weight >1000).

10. **Whole-cell patch pipette delivery:** Similar to microinjection in applicability with the additional capacity for simultaneous imaging and electrophysiological measurements (Eilers and Konnerth, 2000). Inward diffusion of solutes from the patch pipette allows precise control of the intracellular environment but outward diffusion of cytoplasmic contents may be deleterious.

A selection of probes with proven utility for general characterization of living specimens using simple and rapid labeling protocols is listed in Table 17.3.

Tissues

Scientific imperatives allied to technical developments such as two-photon excitation and confocal endoscopy (Helmchen, 2002) mean that fluorescence microscopy is increasingly being applied to tissues and entire organisms. Most of the techniques described above can be adapted for application to tissue specimens, while GFP expression can be confined to specific cell types by coupling to tissue-specific promoters (Hara *et al*., 2003). Water-soluble dyes such as FM 1-43 and lucifer yellow CH generally show deeper penetration into tissues than non-polar molecules such as AM esters, which tend to accumulate in the superficial cell layers (Takahashi *et al*., 2002). A modification of the AM ester technique, referred to as multi-cell bolus loading (MCBL), utilizes localized ejection of small volumes (~0.4 nL) of dye loading solution from a micropipette to label populations of neurons in brain tissue (Stosiek *et al*., 2003). For imaging tissues *in situ*, probe delivery is typically accomplished via the internal pathways of the digestive (Farber *et al*., 2001), respiratory (Lombry *et al*., 2002), circulatory (Ballou *et al*., 2004), or nervous (Grutzendler *et al*., 2003) systems.

Target Abundance and Autofluorescence Considerations

We have considered spectroscopic properties relating to the fluorescence output of labels such as excitation wavelength, exctinction coefficent, photobleaching, and fluorescence quantum yield. However, factors such as the abundance and spatial distribution of the target and the levels of background autofluorescence often have more impact on the contrast and resolution of the final image. The abundance and degree of localization of the target within the specimen are critical determinants in probe selection. For example, it is much easier to image DNA localized in the nucleus than receptors distributed on the plasma membrane surface. The DNA content of a typical mammalian cell is about 7 pg, corresponding to about 6×10^9 base pairs. This amount of DNA can accommodate the binding of up to 1.2×10^9 intercalating dyes (1 dye: 5 base pairs). Consequently, nuclear stains such as propidium iodide (PI) are easily detectable despite the fact that the fluorescence intensity per dye is relatively modest ($\varepsilon_{max} \sim 5000\,M^{-1}cm^{-1}$ and QY ~ 0.1). In contrast, detection of cell-surface EGF receptors, present at ~10,000 copies/cell, by confocal microscopy may require the use of fluorophores such as R-phycoerythrin ($\varepsilon_{max} \sim 1{,}960{,}000\,M^{-1}cm^{-1}$ and QY ~ 0.82) to generate sufficient signal (Good *et al*., 1992). Similar considerations apply when simultaneously imaging two targets using a single excitation wavelength. Typically it is quite difficult to find two dyes that can be excited with equal efficiency at the selected wavelength and also have

TABLE 17.3. Dyes for Rapid Assessment of Living Cells by Fluorescence Microscopy

	Labeling Target	Incubation Concentration[a]	Ex/Em[b]	Laser Lines[c]	GFP Compatible[d]
Hoechst 33342	Nucleus	1 µM*	350/460	351–364 nm or 405 nm	Y
Calcein AM	Cytosol[e]	2 µM*	494/515	488 nm	N
FM 4-64	Plasma membrane, endosomes	5 µM*	506/750[f]	488 nm, 514 nm, or 568 nm	Y
Propidium iodide	Nucleus (dead cells)[g]	5 µM*	535/620	488 nm or 514 nm	Y
LysoTracker Red DND-99	Lysosomes	50 nM	575/590	568 nm	Y
MitoTracker Red CMXRos	Mitochondria	50 nM	578/600	568 nm	Y
AlexaFluor 594 hydrazide	Water (fluid phase tracer)	10 mM[h]	588/615	568 nm	Y

[a] These dyes can generally be used to stain live eukaryotic cells by incubation for 15 to 30 min at the indicated concentration. Dyes marked with an asterisk (*) can be imaged directly in the dye incubation medium, without a subsequent wash step.
[b] Fluorescence excitation/emission maxima in nanometers.
[c] Laser lines suitable for excitation.
[d] Y, fluorescence emission is spectrally well resolved from that of GFP.
[e] Fluorescence is dependent on cytosolic esterase activity and is therefore positively correlated with cell viability.
[f] The fluorescence emission of FM 4-64 has a wide spectral bandwidth and can be detected anywhere from 625 to 800 nm.
[g] Propidium iodide is impermeant to live cells; fluorescence is therefore inversely correlated with cell viability.
[h] Used to fill cells (typically neurons) via microinjection of a 10 mM aqueous solution. Lucifer yellow CH excited at 405 nm is a widely used alternative but is not spectrally well resolved from GFP.

emission spectra that are sufficiently well separated to be discriminated without resorting to spectral unmixing (Fig. 17.2) or the use of quantum dot labels. In this situation, the less efficiently excited dye should be used to detect the more abundant target, thereby equalizing the two emission signals.

Bulk loading procedures, such as AM ester loading, generate intracellular concentrations of up to 100 μ*M*, corresponding to about 1×10^8 molecules in the cytoplasm of a typical mammalian culture cell with a total volume of 4000 μm^3 (of which about 50% is occupied by organelles). Perhaps of more immediate concern to the experimentalist is the cell-to-cell concentration uniformity. A confocal imaging study of neuroblastoma cells loaded with fura-2, AM by Fink and colleagues (1998) found a mean intracellular dye concentration of 38 μ*M* in 123 cells, with individual cell values ranging from 10 to 90 μ*M*. Self-referencing, ratiometric measurements are often used to correct for variability of dye concentration when making cell-to-cell comparisons of fluorescence intensity. Similar intracellular concentrations are achieved in typical microinjection protocols in which 10 m*M* dye solution equivalent to about 1% of cell volume is injected. Much higher concentrations can be attained in situations where probes are sequestered in subcellular compartments. For example, potential-driven uptake of cationic dyes in mitochondria can result in concentrations that are up to 1000-fold higher than in the cytosol (Nicholls and Ward, 2000). These probes should therefore be applied at very low external concentrations (<10 n*M*) to avoid fluorescence self-quenching and respiratory inhibition effects (Rottenberg and Wu, 1998).

The minimum concentration of cytoplasmic EGFP required to be detectable above autofluorescence is about 0.2 μ*M* (Patterson *et al*., 1997), equivalent to about 200,000 copies per cell. This is considerably above the native expression levels of many cellular proteins (range, ~50 – 10^7 copies per cell), making it necessary to overexpress GFP fusion proteins to obtain detectable fluorescence levels. Much lower copy numbers can be detected in restricted volumes. For example, viral particles (~100 nm diameter) containing 120 GFP fusion proteins each are detectable both in isolation and after uptake into cells (Charpilienne *et al*., 2001). Because the number of GFP molecules in these particles is genetically prescribed, they provide useful standards for quantitation of intracellular GFP expression levels (Dundr *et al*., 2002).

Autofluorescence is often the limiting factor that determines how many probe molecules must be introduced into a cell in order to be detectable above background. The autofluorescence of a single 3T3 fibroblast cell has been estimated to be equivalent to about 34,000 fluorescein molecules (Roederer and Murphy, 1986). Surveys of spectral data (Billinton and Knight, 2001; DaCosta *et al*., 2003) show that autofluorescence originates from a wide variety of molecular sources and generally decreases at longer wavelengths. Autofluorescence levels also depend on cell or tissue type and physiological status (Croce *et al*., 1999). For example, lipofuscin, a heterogeneous complex of lipids and proteins found in brain tissues, increases in prevalence with age and the extent of oxidative metabolism (Haralampus-Grynaviski *et al*., 2003). The fluorescence excitation (400–550 nm) and emission (550–750 nm) spectra of lipofuscin are broad, overlapping with many common probes including GFP (Doyle *et al*., 2003). Other significant sources of autofluorescence are NADH/NADPH, flavins, and flavoproteins in mammalian cells, chlorophylls and flavonoids in plants, and collagen and elastin in connective tissues.

Components of culture media such as riboflavin (excitation, 450–490 nm; emission, 500–560 nm) are also significant sources of autofluorescence. The use of minimal media such as Hank's balanced salt solution (HBSS) or media with low riboflavin content such as Ham's F12 is often preferable for live-cell fluorescence imaging. Phenol Red, included as a pH indicator in common culture media, sometimes causes significant quenching of fluorescence. Phenol Red-free media are available from most commercial suppliers of culture media. To provide pH monitoring for cells cultured in Phenol Red-free medium, it is useful to prepare parallel control cultures in conventional Phenol Red-containing medium. A significant technical advance in dealing with autofluorescence problems is the advent of microscopes with spectral analysis and linear unmixing capabilities, which allow probe and autofluorescence background signals to be resolved based on their different spectral fingerprints (Dickinson *et al*., 2001). Likewise, fluorescence lifetime analysis (FLIM) can also sometimes be of use for this purpose. Multi-photon excitation can produce an additional type of background signal in the form of scattered second and third harmonic generation signals (SHG, THG; see Chapter 40, *this volume*). SHG and THG signals are in the visible range at exactly 1/2 or 1/3 of the excitation wavelength. Their production does not depend on the absorption and re-emission of photons but purely on structural features: usually ordered structures such as collagen and cellulose for SHG and surface features for THG. Although the emission of SHG and THG is very strongly oriented in the direction of the beam, in scattering specimens some photons can still be deflected towards the detector.

INTERACTIONS OF PROBES AND SPECIMENS

Once labeling of the specimen is complete, it is imperative that the probe should display appropriate localization for the duration of the planned imaging experiments. Furthermore, the presence of the probe should perturb the normal physiology and structure of the cell or tissue as little as possible.

Localization and Metabolism

As previously discussed, the association between a probe and its target is critical to the accurate representation of the biological properties of the specimen in a fluorescence image. This association is obtained by a variety of mechanisms, some more target-specific than others. The majority of fluorescent probes are labeled analogs of proteins, peptides, lipids, nucleotides, and other biomolecules. In these cases, there is the potential for perturbations to native distribution and activity induced by the attachment of the fluorescent label. However, despite the fact that fluorescent dyes and proteins are not insignificantly small relative to the molecules to which they are attached, their presence is usually tolerated surprisingly well. For example, there are very few examples reported in the literature of aberrant localization of GFP fusion proteins (Katz *et al*., 1998; Unkila *et al*., 2001; Lim *et al*., 2002).

Many dye-based probes, such as nucleic acid stains, ion indicators, and mitochondrial markers are not direct biomolecular analogs. The behavior of these probes is better represented in terms of molecular pharmacology than cell biology. Like therapeutic drugs, their distribution is determined by a combination of several factors including the applied external concentration and rates of transmembrane transport and intracellular metabolism (Fig. 17.5). The staining pattern obtained is usually quite time-dependent and sensitive to factors such as temperature and removal of extracellular dye by washing (Lemasters *et al*., 1999). This can lead to situations such as that depicted in Figure 17.6, where most of the fluorescent labeling is insensitive to the physiological process that it was intended to detect. Another example is provided by non-fluorescent dihydrorhodamine 123, which is oxidized intracellu-

larly by reactive oxygen species (ROS) such as superoxide, hydrogen peroxide, and hydroxyl radicals. The product of this reaction is the cationic fluorescent dye rhodamine 123. It could be concluded from the resulting mitochondrially localized fluorescence that mitochondrially localized ROS generation is being detected when in fact that localization reflects the redistribution of rhodamine 123 from the cytosol to mitochondria (Diaz *et al*., 2003). Many dyes are susceptible to extrusion by active transporters such as the ATP binding cassette (ABC) protein superfamily. Transport rates are governed by transporter substrate specificity and are therefore quite dependent on the molecular structure of the dye (Passamonti and Sottocasa, 1988; Wadkins and Houghton, 1995; Loetchutinat *et al*., 2003). Inhibitors such as sulfinpyrazone, probenecid, MK571, and verapamil can be used to stabilize intracellular dye retention (Di Virgilio *et al*., 1990). Dye extrusion can be advantageously exploited to monitor transporter activity and distribution (weak cellular staining corresponds to high transporter activity) (Hollo *et al*., 1994; Martin *et al*., 2003; Breen *et al*., 2004). In contrast, experiments designed to track the distribution of cell populations in tissues and organisms during processes such as embryological development demand stable and innocuous incorporation of dyes. Dyes useful in these applications are irreversibly coupled to proteins [e.g., carboxyfluoresceindiacetate, succinimidyl ester (CFSE); Parish, 1999] embryological or inert dextran carriers, or are incorporated into membrane lipids (e.g., DiI).

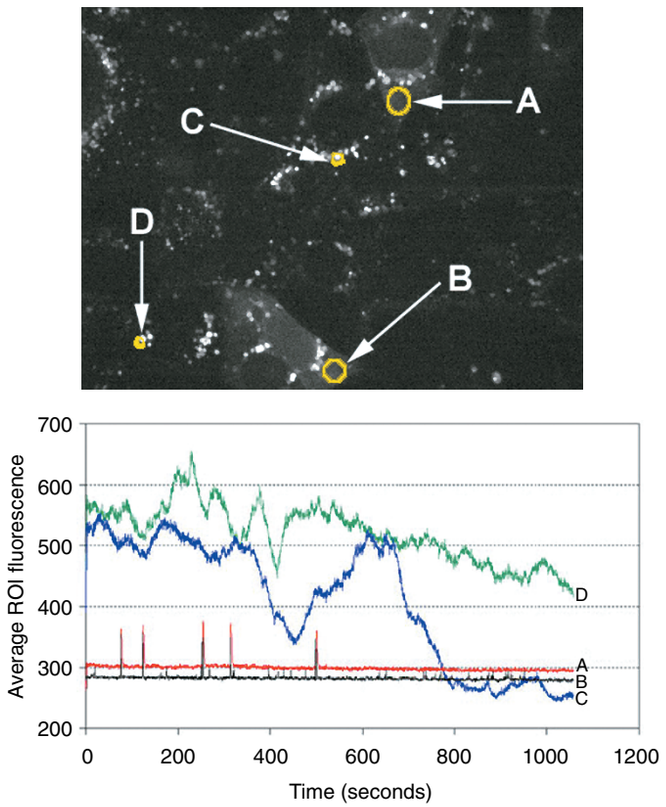

FIGURE 17.6. (Top panel) HL-1 cardiomyocytes (White *et al*., 2004) loaded by incubation with the fluo-4, AM as represented schematically in Figure 17.5. The bright, punctate labeling is due to compartmentalized dye. Cytosolic labeling is faint, diffuse, and only marginally visible in this image. The image was acquired using a PerkinElmer UltraView laser-scanning confocal microscope with a 60×, 1.2 NA, water immersion objective (pixel size = 0.4 µm). (Bottom panel) Photometric traces representing the average fluorescence intensities in the regions of interest A–D (A) as a function of time. The cytosolic regions of two different cells (A and B) exhibit synchronized Ca^{2+} spikes associated with the spontaneous contractile activity of the cells. No systematic variation of Ca^{2+} is detected by the compartmentalized dye (C and D).

Perturbation and Cytotoxicity

Compared to electron microscopy, specimen preparation for fluorescence microscopy is relatively non-invasive. Nevertheless, the concentrations of extrinsic probes required for practical applications are not insignificant in relation to physiological concentrations. Consequently, control experiments to verify that observations are independent of the applied probe concentration are always worthwhile. Severe dye-induced structural and physiological perturbations result in cytotoxicity and cell death. As one might intuitively expect, the most pronounced cytotoxic and perturbative effects tend to be exerted by dyes that accumulate in the organelles most essential to respiration and replication — the mitochondrion and the nucleus. Concentrations of cyanine dyes such as $DiOC_6(3)$ as low as 10 n*M* cause significant inhibition of mitochondrial respiration (Rottenberg and Wu, 1998; Scorrano *et al*., 1999). Subtoxic doses (1–10 µ*M*) of the DNA-binding dye Hoechst 33342 cause increased luciferase gene expression in transfected myocytes (Zhang and Kiechle, 2003). Conversely, probes that are diffusely distributed in the cytosol or the plasma membrane are relatively non-cytotoxic. Cells labeled with CFSE continue to divide and the ensuing bipartition of cellular fluorescence intensity provides a direct indication of proliferation (Parish, 1999). The utility of calcein AM labeling for monitoring cell adhesion and migration derives from its benign effects on these functional properties (De Clerck *et al*., 1994).

A significant concern in the application of GFP chimeras is the need, in some cases, to overexpress a fusion protein in order to achieve detectability over the autofluorescence background. Although overexpression is not usually cytotoxic, it may induce abnormal growth or physiology (Gunjan *et al*., 1999; Wendland and Bumann, 2002). In some cases, cytotoxicty of GFP has been found to be due to products of adjacent expression vector sequences (Endemann *et al*., 2003). Despite their disruptive potential, cytotoxic and perturbative effects of probes are almost always manageable. Even notoriously cytotoxic probes such as dye-labeled phallotoxins can still be used effectively in living cells if the applied concentration is sufficiently low (Pu *et al*., 2000).

UNDER THE MICROSCOPE

Photobleaching

Photobleaching and phototoxicity are two aspects of the same underlying process — generation of reactive oxygen species (ROS) in the specimen as a by-product of fluorescence excitation. Both are of particular concern in prolonged imaging experiments such as long time-lapse sequences. Although photobleaching is usually problematic, resulting in an effective time-dependent decrease in fluorophore concentration, it can be turned to advantage in some cases. Examples include the use of FRAP (fluorescence recovery after photobleaching) to measure diffusion rates and acceptor photobleaching to establish no-transfer reference points in FRET microscopy (Jales-Erijman and Jovin, 2003). With single-photon excitation, the rate of photobleaching and the rate of fluorescence emission are usually both linear functions of excitation intensity. The primary causative mechanism appears to be photosensitization of singlet oxygen ($^1O_2$) generation by the dye triplet excited state (Gandin *et al*., 1983; Song *et al*., 1996;

Eggeling *et al*., 1999; Stracke *et al*.,1999; Gaigalas *et al*., 2002). Singlet oxygen is a highly reactive transient species with a lifetime of about 4 μs in water. In cells, the lifetime of $^1O_2$ is reduced to <0.5 μs due to the increased number of reactive targets presented by proteins and nucleic acids. Therefore, the radius of action of $^1O_2$ is limited to <50 nm from its point of origin. The short range of this effect may be important when "acceptor photobleaching" is used as a rough measure of FRET (see also Chapter 45, *this volume*), because $^1O_2$ produced by excitation of the acceptor is just as likely to bleach any nearby donor. Reaction of $^1O_2$ with dyes generally results in irreversible severance of the conjugated π-electron system responsible for fluorescence.

The extent of photobleaching can be lessened by adjusting any of the three participants in the reaction — excitation light, dye, and oxygen. Decreasing excitation light levels, in both intensity and duration, offers the most direct and consistently effective approach. The intrinsic photostability of organic dyes varies widely depending on their molecular structure (Eggeling *et al*., 1999; Kanofsky and Sima, 2000). The photobleaching quantum yield (the number of photobleaching events per photon absorbed) provides a quantitative expression of propensity for photobleaching. The ratio of the fluorescence quantum yield to the photobleaching quantum yield represents the average number of fluorescence photons generated by a dye before it is photobleached. For fluorescein, this ratio is about 30,000 whereas for rhodamine dyes it is >100,000. Although tabulations of photobleaching quantum yields (Eggeling *et al*., 1999) provide useful guidance, photobleaching rates are also dependent on environmental factors. For example, dye–dye interactions, such as those induced by attaching multiple dyes to a protein, result in increased rates of photobleaching relative to the free monomeric dye (Byers *et al*., 1976; Song *et al*., 1995, 1997). This may account at least partly for the photostability of protein conjugates labeled with AlexaFluor dyes, which are designed to minimize dye–dye interactions via electrostatic repulsion. The availability of reactive oxygen species (primarily $^1O_2$) contributing to photobleaching can be reduced by addition of scavengers, commonly referred to as antifade reagents, to the specimen. Several effective antifade formulations are commercially available; unfortunately these are only applicable to fixed specimens (Berrios *et al*., 1999). Furthermore, antifade reagents may cause fluorescence quenching in addition to attenuation of photobleaching, yielding only a small net increase in the number of photons available for detection (Eggeling *et al*., 1999; see also Chapter 39, *this volume*). Some live cell-compatible antifade reagents have been reported in the literature including Trolox (an analog of vitamin E), ascorbic acid and enzymatic deoxygenation systems (e.g., Oxyrase; Oxyrase Inc., Mansfield, OH; Adler, 1990). However their usage appears to be rather sporadic, suggesting that they are not consistently effective.

Photobleaching in two-photon microscopy is fundamentally a rather different problem than in the one-photon excitation case. The extraordinarily high spatial and temporal confinement of excitation photons required to achieve two-photon excitation (Zipfel *et al*., 2003a) potentially opens photobleaching reaction pathways that are not accessible through one-photon excitation. Whereas the rate of two-photon excited fluorescence emission increases as the square of excitation intensity (I^2), photobleaching rates show higher order ($I^{>2}$) increases (Patterson and Piston, 2000; Dittrich and Schwille, 2001). Analysis by fluorescence correlation spectroscopy (FCS) indicates that the reaction pathways are distinct from photobleaching arising from one-photon excitation in that they do not involve dye triplet excited states (Dittrich and Schwille, 2001).

Phototoxicity

To a large extent, phototoxicity and photobleaching go hand-in-hand. Phototoxicity results from damage exerted by photogenerated reactive oxygen species on proteins, nucleic acids, and other cellular components. Photodamage is usually restricted to the near vicinity of the sensitizer due to the limited diffusional range of $^1O_2$ (Greenbaum *et al*., 2000). Effects farther afield can occur through the action of secondary ROS initially generated from $^1O_2$ (Ouedraogo and Redmond, 2003). Cell death is only the most extreme manifestation of phototoxicity. Other effects may be much more subtle, such as photoinduction of intracellular Ca^{2+} release (Knight *et al*., 2003) or failure to divide.

Although phototoxicity has many determining factors (Table 17.4), controlling light exposure is the most effective limitation

TABLE 17.4. Factors Influencing Phototoxic Effects

Factor[a]	Trend	References
Excitation wavelength	Longer wavelength produce less photodamage.	Bloom & Webb (1984) Manders *et al*. (1999)
Excitation intensity and duration	Higher power and longer exposure result in more photodamage.[b]	Vigers *et al*. (1988) Oh *et al*. (1999) Schafer & Buettner (1999) Manders *et al*. (1999)
Cell type/status	Larger cells can sustain a higher phototoxic burden. Mitotic cells are particularly susceptible to photodamage.	Schafer & Buettner (1999) Manders *et al*., (1999)
Culture medium	Riboflavin and tryptophan induce phototoxicity.	Stoien & Wang (1974) Grzelak *et al*., (2001)
Dye concentration	Higher concentrations produce more photodamage.	Vigers *et al*. (1988) Oh *et al*. (1999)
Dye type	Cyanines and halogenated xanthenes are particularly phototoxic.	Bunting (1992) Gandin *et al*. (1983) Lee *et al*. (1995)
Dye localization	Calcein and GFP phototoxicity is decreased upon compartmentalization in mitochondria and endoplasmic reticulum, respectively.	Beghetto *et al*. (2000) Haseloff *et al*. (1997)
Antioxidant additives	Ascorbic acid and enzymatic deoxygenation systems reduce photoxicity.	Bloom & Webb (1984) Vigers *et al*. (1988).

[a] Note that some factors are strongly interdependent, for example, dye localization and dye concentration. [b] These dependences may by highly nonlinear.

strategy (Manders *et al*., 2004). Reduced photodamage and concomitantly increased specimen viability is one of the principal benefits of two-photon excitation. However, as in the case of photobleaching, although the overall phototoxic burden is vastly reduced compared to one-photon excitation, the severity of photodamage in the focal volume is substantially higher (Koester *et al*., 1999; Tirlapur *et al*., 2001; see also Chapter 38, *this volume*).

SUMMARY

An extensive range of dyes and probes, and techniques for incorporating them into living and fixed specimens, has been developed over the past 30 years. This development, allied to complementary advances in optical engineering and image processing, has propelled fluorescence to become the dominant contrast mechanism used in biological microscopy. Fluorescent labeling technology is a much less exact science than physical optics. This situation is a reflection of the fact that labeling technology must interface directly with the morphological and physiological diversity of biological specimens, rather than any intrinsic shortcomings in the technology itself. Nevertheless, understanding the design and implementation of labeling techniques is an essential element in the ultimate objective of deriving biological information from image data. This chapter has therefore endeavored to assemble a fraction of the extensive and diverse knowledge base on fluorescent probe techniques in one place, with the aim of facilitating critical evaluations of labeling strategies by experimenters.

ACKNOWLEDGMENTS

My thanks to Henry Haeberle (UCSF) and John Jordan (PerkinElmer Life and Analytical Sciences) for their collaboration in the experiments shown in Figure 17.6, which were carried out at the 2004 International 3D Microscopy of Living Cells course (University of British Colombia).

REFERENCES

Adamczyk, M., Mattingly, P.G., Shreder, K., and Yu, Z., 1999, Surface plasmon resonance (SPR) as a tool for antibody conjugate analysis, *Bioconjug. Chem.* 10:1032–1037.

Adams, S.R., Campbell, R.E., Gross, L.A., Martin, B.R., Walkup, G.K., Yao, Y., Llopis, J., and Tsien, R.Y., 2002, New biarsenical ligands and tetracysteine motifs for protein labeling in vitro and in vivo: synthesis and biological applications, *J. Am. Chem. Soc.* 124:6063–6076.

Adler, H.I., 1990, The use of microbial membranes to achieve anaerobiosis, *Crit. Rev. Biotechnol.* 10:119–127.

Ballou, B., Lagerholm, B.C., Ernst, L.A., Bruchez, M.P., and Waggoner, A.S., 2004, Noninvasive imaging of quantum dots in mice, *Bioconjug. Chem.* 15:79–86.

Beghetto, C., Renken, C., Eriksson, O., Jori, G., Bernardi, P., and Ricchelli, F., 2000, Implications of the generation of reactive oxygen species by photoactivated calcein for mitochondrial studies, *Eur. J. Biochem.* 267:5585–5592.

Berlier, J.E., Rothe, A., Buller, G., Bradford, J., Gray, D.R., Filanowski, B.J., Telford, W.G., Yue, S., Liu, J., Cheung, C.Y., Chang, W., Hirsch, J.D., Beechem, J.M., Haugland, R.P., and Haugland, R.P., 2003, Quantitative comparison of long-wavelength AlexaFluor dyes to Cy dyes: Fluorescence of the dyes and their conjugates, *J. Histochem. Cytochem.* 51:1699–1712.

Berrios, M., Conlon, K.A., and Colflesh, D.E., 1999, Antifading agents for confocal fluorescence microscopy, *Methods Enzymol.* 307:55–79.

Beste, G., Schmidt, F.S., Stibora, T., and Skerra, A., 1999, Small antibody-like proteins with prescribed ligand specificities derived from the lipocalin fold, *Proc. Natl. Acad. Sci. USA* 96: 1898–1903.

Bestvater, F., Spiess, E., Stobrawa, G., Hacker, M., Feurer, T., Porwol, T., Berchner-Pfannschmidt, U., Wotzlaw, C., and Acker, H., 2002, Two-photon fluorescence absorption and emission spectra of dyes relevant for cell imaging, *J. Microsc.* 208:108–115.

Billinton, N., and Knight, A.W., 2001, Seeing the wood through the trees: a review of techniques for distinguishing green fluorescent protein from endogenous autofluorescence, *Anal. Biochem.* 291:175–197.

Bloom, J.A., and Webb, W.W., 1984, Photodamage to intact erythrocyte membranes at high laser intensities: methods of assay and suppression, *J. Histochem. Cytochem*. 32:608–616.

Breen, C.M., Sykes, D.B., Baehr, C., Fricker, G., and Miller, D.S., 2004, Fluorescein-methotrexate transport in rat choroid plexus analyzed using confocal microscopy, *Am. J. Physiol.* 287:F562–F569.

Brelje, T.C., Wessendorf, M.W., and Sorenson, R.L., 2002, Multicolor laser scanning confocal immunofluorescence microscopy: Practical application and limitations, *Methods Cell Biol.* 70:165–244.

Bruchez, M. Jr, Moronne, M., Gin, P., Weiss, S., and Alivisatos, A.P., 1998, Semiconductor nanocrystals as fluorescent biological labels, *Science* 281:2013–2016.

Bunting, J.R., 1992, A test of the singlet oxygen mechanism of cationic dye photosensitization of mitochondrial damage, *Photochem. Photobiol.* 55: 81–87.

Byers, G.W., Gross, S., and Henrichs, P.M., 1976, Direct and sensitized photooxidation of cyanine dyes, *Photochem. Photobiol.* 23:37–43.

Campbell, R.E., Tour, O., Palmer, A.E., Steinbach, P.A., Baird, G.S., Zacharias, D.A., and Tsien, R.Y., 2002, A monomeric red fluorescent protein, *Proc. Natl. Acad. Sci. USA* 99:7877–7882.

Cao, F., Eckert, R., Elfgang, C., Nitsche, J.M., Snyder, S.A., Hulser, D.F., Willecke, K., and Nicholson, B.J., 1998, A quantitative analysis of connexin-specific permeability differences of gap junctions expressed in HeLa transfectants and Xenopus oocytes, *J. Cell Sci.* 111:31–43.

Chakrabarti, R., Pfeiffer, N.E., Wylie, D.E., and Schuster, S.M., 1989, Incorporation of monoclonal antibodies into cells by osmotic permeabilization: effect on cellular metabolism, *J. Biol. Chem.* 264:8214–8221.

Chalfie, M., and Kain, S., eds., 1998, *Green Fluorescent Protein: Properties, Applications and Protocols*, Wiley-Liss, New York.

Chan, W.C., and Nie, S., 1998, Quantum dot bioconjugates for ultrasensitive nonisotopic detection, *Science* 281:2016–2018.

Charpilienne, A., Nejmeddine, M., Berois, M., Parez, N., Neumann, E., Hewat, E., Trugnan, G., and Cohen, J., 2001, Individual rotavirus-like particles containing 120 molecules of fluorescent protein are visible in living cells, *J. Biol. Chem.* 276:29361–29367.

Coralli, C., Cemazar, M., Kanthou, C., Tozer, G.M., and Dachs, G.U., 2001, Limitations of the reporter green fluorescent protein under simulated tumor conditions, *Cancer Res* 61:4784–4790.

Croce, A.C., Spano, A., Locatelli, D., Barni, S., Sciola, L., and Bottiroli, G., 1999, Dependence of fibroblast autofluorescence properties on normal and transformed conditions. Role of the metabolic activity, *Photochem. Photobiol.* 69:364–374.

DaCosta, R.S., Andersson, H., and Wilson, B.C., 2003, Molecular fluorescence excitation-emission matrices relevant to tissue spectroscopy, *Photochem. Photobiol.* 78:384–392.

Daly, C., and McGrath, J.C., 2003, Fluorescent ligands, antibodies and preoteins for the study of receptors, *Pharmacol. Ther.* 100:101–118.

De Clerck, L.S., Bridts, C.H., Mertens, A.M., Moens, M.M., and Stevens, W.J., 1994, Use of fluorescent dyes in the determination of adherence of human leucocytes to endothelial cells and the effect of fluorochromes on cellular function, *J. Immunol. Methods* 172:115–124.

Denk, W., Strickler, J.H., and Webb, W.W., 1990, Two-photon laser scanning fluorescence microscopy, *Science* 248:73–76.

Derfus, A.M., Chan, W.C.W., and Bhatia, S.N., 2004, Probing the cytotoxicity of semiconductor quantum dots, *Nano. Lett*. 4:11–18.

Diaz, G., Liu, S., Isola, R., Diana, A., and Falchi, A.M., 2003, Mitochondrial localization of reactive oxygen species by dihydrofluorescein probes, *Histochem. Cell Biol.* 120:319–325.

Dickinson, M.E., Bearman, G., Tille, S., Lansford, R., and Fraser, S.E., 2001, Multi-spectral imaging and linear unmixing add a whole new dimension to laser scanning fluorescence microscopy, *Biotechniques* 31:1272–1278.

Dickinson, M.E., Simbuerger, E., Zimmermann, B., Waters, C.W., and Fraser, S.E., 2003, Multiphoton excitation spectra in biological samples, *J. Biomed. Opt.* 8:329–338.

Dittrich, P.S., and Schwille, P., 2001, Photobleaching and stabilization of fluorophores used for single molecule analysis with one- and two-photon excitation, *Appl. Phys. B* 73:829–837.

Di Virgilio, F., Steinberg T.H., and Silverstein, S.C., 1990, Inhibition of fura-2 sequestration and secretion with organic anion transport blockers, *Cell Calcium* 11:57–62.

Doyle, K.P., Simon, R.P., Snyder, A., and Stenzel-Poore, M.P., 2003, Working with GFP in the brain. *BioTechniques* 34:492–494.

Dundr, M., McNally, J.G., Cohen, J., and Mistelli, T., 2002, Quantitation of GFP-fusion proteins in single living cells, *J. Struct. Biol.* 140:92–99.

Eggeling, C., Widengren, J., Rigler, R., and Seidel C.A.M., 1999, In: *Applied Fluorescence in Chemistry, Biology and Medicine* (W. Rettig, B. Strehmel, S. Schrader, and H. Seifert, eds.), Springer-Verlag, Berlin, pp. 193–240.

Eilers, J., and Konnerth, A., 2000, Dye loading with patch pipets, In: *Imaging Neurons. A Laboratory Manual* (R. Yuste, F. Lanni, and A. Konnerth, eds.), Cold Spring Harbor Laboratory Press, Cold Spring Harbor, New York, pp. 35.1–35.10.

Endemann, G., Schechtman, D., and Mochly-Rosen, D., 2003, Cytotoxicity of pEGFP vector is due to residues encoded by multiple cloning site, *Anal. Biochem.* 313:345–347.

Farber, S.A., Pack, M., Ho, S.Y., Johnson, I.D., Wagner, D.S., Dosch, R., Mullins, M.C., Hendrickson, H.S., Hendrickson, E.K., and Halpern, M.E., 2001, Genetic analysis of digestive physiology using fluorescent phospholipid reporters, *Science* 292:1385–1388.

Farinas, J., and Verkman, A.S., 1999, Receptor-mediated targeting of fluorescent probes in living cells, *J. Biol. Chem.* 274:7603–7606.

Fink, C., Morgan, F., and Loew, L.M., 1998, Intracellular fluorescent probe concentrations by confocal microscopy, *Biophys. J.* 75:1648–1658.

Fischer, P.M., Krausz, E., and Lane, D.P., 2001, Cellular delivery of impermeable effector molecules in the form of conjugates with peptides capable of mediating membrane translocation, *Bioconj. Chem.* 12:825–841.

Fricker, M.D., and Meyer, A.J., 2001, Confocal imaging of metabolism in vivo: Pitfalls and possibilities, *J. Exp. Bot.* 52:631–640.

Gaigalas, A.K., Wang, L., and Vogt, R.F., 2002, Frequency-domain measurement of the photodegradation process of fluorescein, *Photochem. Photobiol.* 76:22–28.

Gan, B.S., Krump, E., Shrode, L.D., and Grinstein, S., 1998, Loading pyranine via purinergic recepetors or hypotonic stress for measurement of cytosolic pH by imaging, *Am. J. Physiol.* 275: C1158–C1166.

Gandin, E., Lion, Y., and Van de Vorst, A., 1983, Quantum yield of singlet oxygen production by xanthene derivatives, *Photochem. Photobiol.* 37:271–278.

Gerhardt, G.A., and Palmer, M.R., 1987, Characterization of the techniques of pressure ejection and microiontophoresis using in vivo electrochemistry, *J. Neurosci. Methods* 22:147–159.

Good, M.J., Hage, W.J., Mummery, C.L., De Laat, S.W., and Boonstra, J., 1992, Localization and quantification of epidermal growth factor receptors on single cells by confocal laser scanning microscopy, *J. Histochem. Cytochem.* 40:1353–1361.

Greenbaum, L., Rothmann, C., Lavie, R., and Malik Z., 2000, Green fluorescent protein photobleaching: A model for protein damage by endogenous and exogenous singlet oxygen, *Biol. Chem.* 381:1251–1258.

Grzelak, A., Rychlik, B., and Bartosz, G., 2001, Light-dependent generation of reactive oxygen species in cell culture media, *Free Radic. Biol. Med.* 30:1418–1425.

Grutzendler, J., Tsai, J., and Gan, W.G., 2003, Rapid labeling of neuronal populations by ballistic delivery of fluorescent dyes, *Methods* 30:79–85.

Gunjan, A., Alexander, B.T., Sittman, D.B., and Brown, D.T., 1999, Effects of H1 histone variant overexpression on chromatin structure, *J. Biol. Chem.* 274:37950–37956.

Haas, K., Sin, W.-C., Javaherian, A., Li, Z., and Cline, H.T., 2001, Single-cell electroporation for gene transfer in vivo, *Neuron* 29:583–591.

Hara, M., Wang, X., Kawamura, T., Bindokas, V.P., Dizon, R.F, Alcoser, S.Y., Magnuson, M.A., and Bell, G.I., 2003, Transgenic mice with green fluorescent protein–labeled pancreatic β-cells, *Am. J. Physiol.* 284:E1177–E1183.

Haralampus-Grynaviski, N.M., Lamb, L.E., Clancy, C.M., Skumatz, C., Burke, J.M., Sarna, T., and Simon, J.D., 2003, Spectroscopic and morphological studies of human retinal lipofuscin granules, *Proc. Natl. Acad. Sci. USA* 100:3179–3184.

Haseloff, J., Siemering, K.R., Prasher, D.C., and Hodge, S., 1997, Removal of a cryptic intron and subcellular localization of green fluorescent protein are required to mark transgenic Arabidopsis plants brightly, *Proc. Natl. Acad. Sci. USA* 94:2122–2127.

Hashimoto, K., Tatsumi, N., and Okada, K., 1989, Introduction of phalloidin labelled with fluorescein isothiocyanate into living polymorphonuclear leukocytes by electroporation, *J. Biochem. Biophys. Methods* 19:143–154.

Haugland, R.P., 2002, *Handbook of Fluorescent Probes and Research Products, Ninth Edition,* Molecular Probes, Inc., Eugene, Oregon.

Helmchen, F., 2002, Miniaturization of fluorescence microscopes using fibre optics, *Exp. Physiol.* 87:737–745.

Hermanson, G.P., 1996, *Bioconjugate Techniques,* Academic Press, San Diego, California.

Hollo, Z., Homolya, L., Davis, C.W., and Sarkadi, B., 1994, Calcein accumulation as a fluorometric functional assay of the multidrug transporter, *Biochim. Biophys. Acta* 1191:384–388.

Jaiswal, J.K., Mattoussi, H., Mauro, J.M., and Simon, S.M., 2003, Long-term multiple color imaging of live cells using quantum dot bioconjugates, *Nat. Biotechnol.* 21:47–52.

Jales-Erijman, E.A., and Jovin, T.M., 2003, FRET imaging, *Nat. Biotechnol.* 21:1387–1395.

Kanofsky, J.R., and Sima P.D., 2000, Structural and environmental requirements for quenching of singlet oxygen by cyanine dyes, *Photochem. Photobiol.* 71:361–368.

Katz, B.Z., Krylov, D., Aota, S.I., Olive, M., Vinson, C., and Yamada, K.M., 1998, Green fluorescent protein labeling of cytoskeletal structures — Novel targeting approach based on leucine zippers, *BioTechniques* 25: 298–304.

Knight, M.M., Roberts, S.R., Lee, D.A., and Bader, D.L., 2003, Live cell imaging using confocal microscopy induces intracellular calcium transients and cell death, *Am. J. Physiol.* 284:C1083–C1089.

Koester, H.J., Baur, D., Uhl, R., and Hell, S.W., 1999, Ca^{2+} fluorescence imaging with pico- and femtosecond two-photon excitation: signal and photodamage, *Biophys. J.* 77:2226–2236.

Larson, D.R., Zipfel, W.R., Williams, R.M., Clark, S.W., Bruchez, M.P., Wise, F.W., and Webb, W.W., 2003, Water soluble quantum dots for multiphoton fluorescence imaging *in vivo*, *Science* 300:1434–1436.

Lee, C., Wu, S.S., and Chen, L.B., 1995, Photosensitization by 3,3′-dihexyloxacarbocyanine iodide: Specific disruption of microtubules and inactivation of organelle motility, *Cancer Res.* 55:2063–2069.

Lemasters, J.J., Trollinger, D.R., Qian, T., Cascio, W.E., and Ohata, H., 1999, Confocal imaging of Ca^{2+}, pH, electrical potential and membrane permeability in single living cells, *Methods Enzymol.* 302:341–358.

Lim, M.L., Lum, M.G., Hansen, T.M., Roucou, X., and Nagley, P., 2002, On the release of cytochrome c from mitochondria during cell death signaling, *J. Biomed. Sci.* 9:488–506.

Lippincott-Schwartz, J., and Patterson, G.H., 2003, Development and use of fluorescent protein markers in living cells, *Science* 300:87–91.

Loetchutinat, C., Saengkhae, C., Marbeuf-Gueye, C., and Garnier-Suillerot, A., 2003, New insights into the P-glycoprotein-mediated effluxes of rhodamines, *Eur. J. Biochem.* 270:476–485.

Lombry, C., Bosquillon, C., Preat, V., and Vanbever, R., 2002, Confocal imaging of rat lungs following intratracheal delivery of dry powders or solutions of fluorescent probes, *J. Controlled Release* 83:331–341.

Lu, J., and Zenobi, R., 2000, *In-situ* monitoring of protein labeling reactions by matrix-assisted laser desorption/ionization mass spectrometry, *Fresnius J. Anal. Chem.* 366:3–9.

Manders, E.M., Kimura, H., and Cook, P.R., 1999, Direct imaging of DNA in living cells reveals the dynamics of chromosome formation, *J. Cell Biol.* 144:813–821.

Manders, E., Van Oven, C., and Hoebe, R., 2004, Phototoxicity in live-cell imaging and an effective way to reduce it: Controlled light exposure microscopy (CLEM), In: *Abstracts of Focus on Microscopy 2004 Meeting*.

Marrero, M.B., Schieffer, B., Paxton, W.G., Schieffer, E., and Bernstein, K.E., 1995, Electroporation of pp60*c-src* antibodies inhibits the angiotensin II activation of phospholipase C-γ1 in rat aortic smooth muscle cells, *J. Biol. Chem*. 270:15734–15738.

Martin, C., Walker, J., Rothnie, A., and Callaghan, R., 2003, The expression of P-glycoprotein does influence the distribution of novel fluorescent compounds in solid tumour models, *Br. J. Cancer* 89:1581–1589.

Mattheakis, L.C., Dias, J.M., Choi, Y.J., Gong, J., Bruchez, M.P., Liu, J., and Wang, E., 2004, Optical coding of mammalian cells using semiconductor quantum dots, *Anal. Biochem.* 327:200–208.

Matz M.V., Fradkov, A.F., Labas, Y.A., Savitsky, A.P., Zaraisky, A.G., Markelov, M.L., and Lukyanov, S.A., 1999, Fluorescent proteins from nonbioluminescent Anthozoa species, *Nat. Biotechnol.* 17:969–973.

Mercola, D.A., Morris, J.W.S., and Arquilla, E.R., 1972, Use of resonance interaction in the study of the chain folding of insulin in solution, *Biochemistry* 11:3860–3874.

Meyers, J.R., MacDonald, R.B., Duggan, A., Lenzi, D., Standaert, D.G., Corwin, J.T., and Corey, D.P., 2003, Lighting up the senses: FM1-43 loading of sensory cells through nonselective ion channels, *J. Neurosci.* 23:4054–4065.

Mook, O.R., Van Overbeek C., Ackema, E.G., Van Maldegem, F., and Frederiks, W.M., 2003, In situ localization of gelatinolytic activity in the extracellular matrix of metastases of colon cancer in rat liver using quenched fluorogenic DQ-gelatin, *J. Histochem. Cytochem.* 51:821–829.

Mujumdar, R.B., Ernst, L.A., Mujumdar, S.R., Lewis, C.J., and Waggoner, A.S., 1993, Cyanine dye labeling reagents: Sulfoindocyanine succinimidyl esters, *Bioconjug. Chem.* 4:105–111.

Nemetz, C., Reichhuber, R., Schweizer, R., Hloch, P., and Watzele, M., 2001, Reliable quantification of in vitro synthesized green fluorescent protein: Comparison of fluorescence activity and total protein levels, *Electrophoresis* 22:966–969.

Nicholls, D.G., and Ward, M.W., 2000, Mitochondrial membrane potential and neuronal glutamate excitotoxicity: mortality and millivolts, *Trends Neurosci.* 23:166–174.

O'Brien, J.A, Holt, M., Whiteside, G., Lummis, S.C., and Hastings, M.H., 2001, Improvements to the hand-held Gene Gun: Improvements for in vitro biolistic transfection of organotypic neuronal tissue, *J. Neurosci. Methods* 112:57–64.

Oh, D.J., Lee, G.M., Francis, K., and Palsson, B.O., 1999, Phototoxicity of the fluorescent membrane dyes PKH2 and PKH26 on the human hematopoietic KG1a progenitor cell line, *Cytometry* 36:312–318.

Ouedraogo, G.D., and Redmond, R.W., 2003, Secondary reactive oxygen species extend the range of photosensitization effects in cells: DNA damage produced via initial membrane photosensitization, *Photochem. Photobiol.* 77:192–203.

Pagano, R.E., Watanabe, R., Wheatley, C., and Dominguez, M., 2000, Applications of BOPIDY-sphingolipid analogs to study lipid traffic and metabolism in cells, *Methods Enzymol.* 312:523–534.

Panchuk-Voloshina, N., Haugland, R.P., Bishop-Stewart, J., Bhalgat, M.K., Millard, P.J., Mao, F., Leung, W.-Y., and Haugland, R.P., 1999, Alexa dyes, a series of new fluorescent dyes that yield exceptionally bright, photostable conjugates, *J. Histochem. Cytochem.* 47:1179–1188.

Parish, C.R., 1999, Fluorescent dyes for lymphocyte migration and proliferation studies, *Immunol. Cell Biol.* 77:499–508.

Passamonti, S., and Sottocasa, G., 1988, The quinoid structure is the molecular requirement for recognition of phthaleins by the organic anion carrier at the sinusoidal plasma membrane level in the liver, *Biochim. Biophys. Acta* 943:119–125.

Patterson, G.H., Knobel, S.M., Sharif, W.D., Kain, S.R., and Piston, D.W., 1997, Use of the green fluorescent protein and its mutants in quantitative fluorescence microscopy, *Biophys. J.* 73:2782–2790.

Patterson, G.H., and Piston, D.W., 2000, Photobleaching in two-photon excitation microscopy, *Biophys. J.* 78:2159–2162.

Potocky, T.B., Menon, A.K., and Gellman, S.H., 2003, Cytoplasmic and nuclear delivery of a TAT-derived peptide and a β-peptide after endocytic uptake into HeLa cells, *J. Biol. Chem.* 278:50188–50194.

Pu, R., Wozniak, M., and Robinson, K.R., 2000, Cortical actin filaments form rapidly during photopolarization and are required for the development of calcium gradients in Pelvetia compressa zygotes, *Dev. Biol.* 222:440–449.

Ramjeesingh, M., Zywulko, M., Rothstein, A., Whyte, R., and Shami, E.Y., 1990, Antigen protection of monoclonal antibodies undergoing labeling, *J. Immunol. Methods* 133:159–167.

Rocheleau, J.V., Head, W.S., and Piston, D.W., 2004, Quantitative NAD(P)H/flavoprotein autofluorescence imaging reveals metabolic mechanisms of pancreatic islet pyruvate response, *J. Biol. Chem.* 279: 31780–31787

Roederer, M., and Murphy, R.F., 1986, Cell-by-cell autofluorescence correction for low signal-to-noise systems: Application to epidermal growth factor endocytosis by 3T3 fibroblasts, *Cytometry* 7:558–565.

Rose, C.R., Kovalchuk, Y., Eilers, J., and Konnerth, A., 1999, Two-photon Na^+ imaging in spines and fine dendrites of central neurons, *Pflügers Arch.* 439:201–207.

Rottenberg, H., and Wu, S., 1998, Quantitative assay by flow cytometry of the mitochondrial membrane potential in intact cells, *Biochim. Biophys. Acta* 1404:393–404.

Rubart, M., Wang, E., Dunn, K.W., and Field, L.J., 2003, Two-photon molecular excitation imaging of Ca^{2+} transients in Langendorff-perfused mouse hearts, *Am. J. Physiol. Cell Physiol.* 284:C1654–C1668.

Ruthazer, E.S., and Cline, H.T., 2002, Multiphoton imaging of neurons in living tissue: Acquisition and analysis of time-lapse morphological data, *Real-Time Imaging* 8:175–188.

Schafer, F.Q., and Buettner, G.R., 1999, Singlet oxygen toxicity is cell line-dependent: a study of lipid peroxidation in nine leukemia cell lines, *Photochem. Photobiol.* 70:858–867.

Scorrano, L., Petronilli, V., Colonna, R., Di Lisa, F., and Bernardi, P., 1999, Chloromethyltetramethylrosamine (Mitotracker Orange) induces the mitochondrial permeability transition and inhibits respiratory complex I, *J. Biol. Chem.* 274:24657–24663.

Siegel, R.M., Chan, F.K., Zacharias, D.A., Swofford, R., Holmes, K.L., Tsien, R.Y., and Lenardo, M.J., 2000, Measurement of molecular interactions in living cells by fluorescence resonance energy transfer between variants of the green fluorescent protein, *Science Signal Transduction Knowledge Environment,* available at http://stke.sciencemag.org/cgi/content/full/OC_sigtrans;2000/38/pl1.

Song, L., Hennink, E.J., Young, I.T., and Tanke, H.J., 1995, Photobleaching kinetics of fluorescein in quantitative fluorescence microscopy, *Biophys. J.* 68:2588–2600.

Song, L., Varma, C.A., Verhoeven, J.W., and Tanke, H.J., 1996, Influence of the triplet excited state on the photobleaching kinetics of fluorescein in microscopy, *Biophys. J.* 70:2959–2968.

Song, L., van Gijlswijk, R.P., Young, I.T., and Tanke, H.J., 1997, Influence of fluorochrome labeling density on the photobleaching kinetics of fluorescein in microscopy, *Cytometry* 27:213–223.

Stephens, D.G., and Pepperkok, R., 2001, The many ways to cross the plasma membrane, *Proc. Natl. Acad. Sci. USA* 98:4295–4298.

Stoien, J.D., and Wang, R.J., 1974, Effect of near-ultraviolet and visible light on mammalian cells in culture II. Formation of toxic photoproducts in tissue culture medium by blacklight, *Proc. Natl. Acad. Sci. USA* 71:3961–3965.

Storms, M.M.H., Van der Schoot, C., Prins, M., Kormelink, R., Van Lent, J.W.M., and Goldbach, R.W., 1998, A comparison of two methods of microinjection for assessing altered plasmodesmal gating in tissues expressing viral movement proteins, *Plant J.* 13:131–140.

Stosiek, C., Garaschuk, O., Holthoff, K., and Konnerth, A., 2003, *In vivo* two-photon calcium imaging of neuronal networks, *Proc. Natl. Acad. Sci. USA* 100:7319–7324.

Stracke, F., Heupel, M., and Thiel, E., 1999, Singlet molecular oxygen photosensitized by rhodamine dyes: Correlation with photophysical properties of the sensitizers, *J. Photochem. Photobiol. A* 126:51–58.

Sullivan, K.F., and Kay, S.A., eds., 1999, *Green Fluorescent Proteins,* Academic Press, San Diego, California.

Takahashi, N., Nemoto, T., Kimura, R., Tachikawa, A., Miwa, A., Okado, H., Miyashita, Y., Iino, M., Kadowaki, T., and Kasai, H., 2002, Two-photon excitation imaging of pancreatic islets with various fluorescent probes, *Diabetes* 51:S25–S28.

Tanhuanpaa, K., and Somerharju, P., 1999, Gamma-cyclodextrins greatly enhance translocation of hydrophobic fluorescent phospholipids from vesicles to cells in culture. Importance of molecular hydrophobicity in phospholipid trafficking studies, *J. Biol. Chem.* 274:35359–35366.

Tirlapur, U.K., Konig, K., Peuckert, C., Krieg, R., and Halbhuber, K.J., 2001, Femtosecond near-infrared laser pulses elicit generation of reactive oxygen species in mammalian cells leading to apoptosis-like death, *Exp. Cell Res.* 263:88–97.

Tooley, A.J., Cai, Y.A., and Glazer, A.N., 2001, Biosynthesis of a fluorescent cyanobacterial C-phycocyanin holo-alpha subunit in a heterologous host, *Proc. Natl. Acad. Sci. USA* 98:10560–10565.

Tsien, R.Y., 1998, The green fluorescent protein, *Ann. Rev. Biochem.* 67:509–544.

Unkila, M., McColl, K.S., Thomenius, M.J., Heiskanen, K., and Distelhorst, C.W., 2001, Unreliability of the cytochrome c-enhanced green fluorescent fusion protein as a marker of cytochrome c release in cells that overexpress Bcl-2, *J. Biol. Chem.* 276:39132–39137.

Vigers, G.P., Coue, M., and McIntosh, J.R., 1988, Fluorescent microtubules break up under illumination, *J. Cell Biol.* 107:1011–1024.

Wadkins, R.M., and Houghton, P.J., 1995, Kinetics of transport of dialkyloxacarbocyanines in multidrug-resistant cell lines overexpressing P-glycoprotein: Interrelationship of dye alkyl chain length, cellular flux, and drug resistance, *Biochemistry* 34:3858–3872.

Waizenegger, T., Fischer, R., and Brock, R., 2002, Intracellular concentration measurement in adherent cells: A comparison of import efficiencies of cell-permeable peptides, *Biol. Chem.* 383:291–299.

Walev, I., Bhakdi, S.C., Hofmann, F., Djonder, N., Valeva, A., Aktories, K., and Bhakdi, S., 2001, Delivery of proteins into living cells by reversible membrane permeabilization with streptolysin O, *Proc. Natl. Acad. Sci. USA* 98:3185–3190.

Wang, G., Achim, C.L., Hamilton, R.L., Wiley, C.A., and Soontornniyomkij, V., 1999, Tyramide signal amplification method in multiple-label immunofluorescence confocal microscopy, *Methods* 18:459–464.

Watson, A., Wu, X., and Bruchez, M., 2003, Lighting up cells with quantum dots, *BioTechniques* 34:296–303.

Wendland, M., and Bumann, D., 2002, Optimization of GFP levels for analyzing Salmonella gene expression during an infection, *FEBS Lett.* 521:105–108.

White, S.M, Constantin, P.E., and Claycomb, W.C., 2004, Cardiac physiology at the cellular level: use of cultured HL-1 cardiomyocytes for studies of cardiac muscle cell structure and function, *Am. J. Physiol.* 286:H823–H829.

Wu, X., Liu, H., Liu, J., Haley, K.N., Treadway, J.A., Larson, J.P., Ge, N., Peale, F., and Bruchez, M.P., 2003, Immunofluorescent labeling of cancer marker Her2 and other cellular targets with semiconductor quantum dots, *Nat. Biotechnol.* 21:41–46.

Xu, C., and Webb, W.W., 1996, Measurement of two-photon excitation cross sections of molecular fluorophores with data from 690 to 1050 nm, *J. Opt. Soc. Am. B* 13:481–491.

Xu, C., Zipfel, W., Shear, J.B., Williams, R.M., and Webb, W.W., 1996, Multiphoton fluorescence excitation: new spectral windows for biological nonlinear microscopy, *Proc. Natl. Acad. Sci. USA* 93:10763–10768.

Yasuda, K., Momose, T., and Takahashi, Y., 2000, Applications of microelectroporation for studies of chick embryogenesis, *Dev. Growth Differ.* 42:203–206.

Zipfel, W., Williams, R.M., and Webb, W.W., 2003a, Nonlinear magic: Multiphoton microscopy in the biosciences, *Nat. Biotechol.* 21:1369–1377.

Zipfel, W.R., Williams, R.M., Christie, R., Nikitin, A.Y., Hyman, B.T., and Webb, W.W., 2003b, Live tissue intrinsic emission microscopy using multiphoton-excited native fluorescence and second harmonic generation, *Proc. Natl. Acad. Sci. USA* 100:7075–7080.

Zhang, J., Campbell, R.E., Ting, A.Y., and Tsien, R.Y., 2002, Creating new fluorescent probes for cell biology, *Nat. Rev. Mol. Cell Biol.* 3:906–918.

Zhang, X., and Kiechle, F.L., 2003, Hoechst 33342 alters luciferase gene expression in transfected BC3H-1 myocytes, *Arch. Pathol. Lab. Med.* 127:1124–1132.

Zhao, M., Hollingworth, S., and Baylor, S.M., 1997, AM-loading of fluorescent Ca^{2+} indicators into intact fibers of frog muscle, *Biophys. J.* 72:2736–2747.